Coupling of Proton Motions in Catalytic Activated Complexes. Model Potential-Energy Surfaces for Hydrogen-Bond Chains[1]

Richard D. Gandour, Gerald M. Maggiora, and Richard L. Schowen*

Contribution from the Departments of Biochemistry and Chemistry, University of Kansas, Lawrence, Kansas 66045. *Received June 1, 1974*

Abstract: Potential surfaces for proton motion in the systems $^{+}A\text{–}H\cdots BH\cdots A$, where A is H_2O or NH_3 and BH is H_2O or HF, have been calculated by the INDO method for a series of constrained A–B distances. The results, which constitute a model for proton-transfer processes in enzyme catalysis and intramolecular reactions, are *qualitatively interpretable* in terms of a hydrogen-bond building-up principle. According to this principle, energy profiles along the surfaces are built up from component hydrogen-bond potentials. Mechanisms for dual proton transfer to generate $A\cdots H\text{–}B\cdots H\text{–}A^{+}$, which may be important in "charge relay" chains and in multifunctional catalysis, are classified as coupled or uncoupled according to the degree of correlation in motion of the two protons along the reaction path. The coupling is further described as dynamical (if it prevails along the entire reaction path) or kinetic (with reference to reaction-coordinate motion in an activated complex). Uncoupled paths may pass through cationic intermediates ($A\cdots H\text{–}B\text{–}H^{+}\cdots A$) or anionic intermediates ($^{+}AH\cdots B^{-}\cdots HA^{+}$). Calculations were performed for long (A–B $\sim$ 3 Å), medium (A–B $\sim$ 2.75 Å), and short (A–B $\sim$ 2.5 Å) assemblies. In the long systems, the surfaces corresponded throughout to double-minimum hydrogen-bond behavior. All reaction pathways were dynamically and kinetically uncoupled. All short systems produced surfaces corresponding throughout to single-minimum hydrogen-bond behavior so that the only stable structure was a "supermolecule" $A\cdots H\cdots B\cdots H\cdots A$. Medium systems exhibited a great variability in character with reaction pathways and mechanisms highly dependent on chemical factors. Dynamic coupling in these systems arises only when the inherent stability of the cationic and anionic intermediates is very similar; it is accompanied by kinetic coupling. All other circumstances yield dynamically uncoupled mechanisms. Whenever the favored intermediate is a defined species (minimum on the surface), the mechanism is also kinetically uncoupled. Kinetic coupling is found when the reactant-intermediate potential achieves single-minimum character and the intermediate *per se* has no existence.

The catalytic power of enzymes is recognized to originate in a major part from acid–base catalysis, in which the motion of protons in activated complexes counterbalances and facilitates the flow of electrons.[2] A generation and a half of quantitative investigation of acid–base catalysis has now been invested in small-molecule reactions, which can be used to a degree as models for the interactions in enzyme active sites. These models should be accurate insofar as the identity of the functional groups is important, but they lack the geometrical constraints and possibly some environmental characteristics of the enzymic reactions.[2-4] This experience indicates that simple acid–base catalysis, duplicating behavior in model systems, is incapable of accounting for the entirety of enzymic accelerations and that special features, such as a high degree of orientation[4] or a coupling of several catalytic events (multifunctional catalysis),[5] are probably required.

The coupling of catalytic events in enzyme-active sites is a particularly interesting hypothesis, because it is still quite unclear what factors would influence such coupling and thus how molecular evolution might have built the machinery for such catalysis into protein structure.

The simplest kind of such catalytic coupling which can be imagined is the coupling of two proton motions,[6] either in the form of *bifunctional catalysis*[5] (**1**) or of *charge-relay chains*[7] (**2**). In this paper, we report a

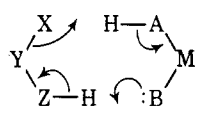

1

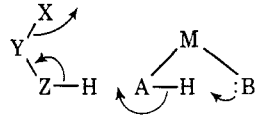

2

theoretical investigation of the factors which affect the degree of coupling of proton motion in the interconversion of the tautomeric forms of the hydrogen-bond chains existing in both **1** and **2**, as exemplified in the reaction of eq 1. The upper and lower structures in

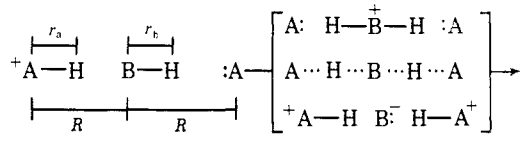

A: H—B H—A^{+} (1)

the middle of the arrow represent species formed in the course of uncoupled proton transfer. Thus simple proton donation to the bridging molecule BH generates the upper structure, while simple proton transfer from the bridge to the acceptor A generates the lower struc-

(1) The research was supported by grants from the National Institutes of Health and the National Science Foundation, and by a grant of computer time from the University of Kansas. A preliminary report of this work was presented at the 9th Midwest Regional Meeting of the American Chemical Society, Oct 25–26, 1973, Abstract 531.

(2) (a) W. P. Jencks, "Catalysis in Chemistry and Enzymology," McGraw-Hill, New York, N. Y., 1969; (b) M. L. Bender, "Mechanisms of Homogeneous Catalysis from Protons to Proteins," Wiley-Interscience, New York, N. Y., 1971.

(3) T. C. Bruice and S. J. Benkovic, "Bioorganic Mechanisms," W. A. Benjamin, New York, N. Y., 1966.

(4) T. C. Bruice, in "The Enzymes," Vol. 2, 3rd ed, P. D. Boyer, Ed., Academic Press, New York, N. Y., 1970, Chapter 4.

(5) C. G. Swain and F. F. Brown, Jr., *J. Amer. Chem. Soc.*, **74**, 2534, 2538 (1952); P. R. Rony, *ibid.*, **95**, 2896 (1973), and preceding papers; J. P. Li, *Aldrichimica Acta*, **5**, 5 (1972), and references cited therein.

(6) A rather more complex type of coupling has been suggested by N. Ressler, *J. Theor. Biol.*, **23**, 425 (1969) and is based on the coupling of vibrational or electronic resonant energy to proton transfer reactions.

(7) D. M. Blow, J. J. Birktoft, and B. S. Hartley, *Nature (London)*, **221**, 337 (1969).

ture. Both of these intermediate species can be converted to the product by one further, uncoupled proton transfer. The center structure represents the transition state for coupled motion of the two protons.

Our purpose is to examine the *qualitative* effects on the choice of reaction path of two variables, *viz.*, the A–B distance (R in eq 1), and the molecular nature of the donor–acceptor (AH/A) and bridging (BH) species, by calculating the potential-energy surfaces for the motion of the transferring protons as a function of these variables.

Choice of Technique. The INDO all-valence-electron self-consistent field molecular orbital (SCFMO) method was employed in the present calculations.[8] As shown by DePaz, *et al.*,[9] using the closely related CNDO/2 method[10] and by Plummer[11] using the INDO method, the geometric results obtained for $(H_2O)_nH^+$ systems are in reasonable agreement with those obtained by Newton and Ehrenson[12] using *ab initio* techniques. Kollman and Allen[13] have also presented an excellent comparative discussion of the merits and demerits of semiempirical and *ab initio* hydrogen-bond calculations for a wide variety of systems. They find that the CNDO/2 method gives similar qualitative but not quantitative results when compared with *ab initio* calculations. Finally, a second-order perturbation treatment (inclusion of correlation) of hydrogen bonding within the CNDO/2 framework showed that similar qualitative, although not quantitative, results were obtained.[14] Since our aim is to develop qualitative concepts, the INDO method utilized in the present study should produce results of sufficient accuracy to indicate the important *trends* which occur in the different systems investigated.

Because the masses of the AH/A and BH molecular species are much larger than that of the transferring protons, we can approximate the motion of the system by assuming that only the transferring protons move. This approximation essentially neglects the coupling between the proton-transfer modes and the A···B···A stretching modes. Although the neglect of this coupling will not affect conclusions of the type sought in this study, it is true that in quantitative applications, such as the interpretation of infrared spectra,[15-17] such coupling must be considered.

Choice of Structures. As our interest in the present study is primarily in modeling enzyme or large-molecule systems, where the A–B distances are determined by "external" forces[18] which override those of the complex itself, the fixing of the geometry of the AH/A and BH species is a reasonable approximation. The approximate, three-dimensional, adiabatic[19] potential-energy surfaces are then calculated by use of the Born–Oppenheimer or "clamped nuclei" approximation,[20,21] which allows the fixing of *all* nuclear coordinates during the computation of the electronic energy of the system. The surfaces so obtained should provide a reasonable basis for describing the dynamics of the transferring protons. Such two-proton surfaces have been calculated for the nucleic acid base pairs[22-24] and cyclic formamide dimer.[25] The results of these studies have provided valuable insights into the dynamics of coupled proton systems. In order to choose acid–base systems common in enzyme and enzyme-model proton-transfer chains, we selected ammonia (NH_3) and water (H_2O) to represent reasonably basic and reasonably nonbasic proton acceptors, and their conjugate acids, ammonium (NH_4^+) and hydronium (H_3O^+) ions, as weak and strong proton donors. The most common bridging molecule in real systems is doubtlessly water, which was therefore employed in the calculations. To develop the degree to which the results depend on the bridging structure, we also included the least basic and most acidic simple structure, hydrofluoric acid (HF), as a bridge in spite of its rarity in acid–base catalytic systems.

Terminology and Notation. Since we want to construct potential-energy surfaces for the reactions depicted in eq 1, all our systems are "symmetrical," *i.e.*, AH^+ is the proton donor and its conjugate base, A, is the final proton acceptor.

All reactions involve one or more of three possible pathways (eq 2, 3, and 4). A useful shorthand notation for the species is shown under the structures in these equations; in this notation only the heavy atoms and charges are indicated (thus A^+BA for $^+AH\ BH:A$). Equation 2 represents the *coupled pathway* in which both proton motions occur simultaneously. Equations 3a and 3b together represent an uncoupled route, passing through a species involving the cation HBH^+; this will be referred to hereafter as the *cationic pathway*. Equations 4a and 4b together show the other possible uncoupled route, *via* the anion $B:^-$, and we shall call it the *anionic pathway*.

$$\underset{A^+BA}{{}^+A\text{–}H\ B\text{–}H:A} \longrightarrow \underset{ABA^+}{A:\ H\text{–}B\ H\text{–}A^+} \qquad (2)$$

$$\underset{A^+BA}{{}^+A\text{–}H\ B\text{–}H:A} \longrightarrow \underset{AB^+A}{A:\ H\text{–}B^+\text{–}H:A} \qquad (3a)$$

$$\underset{AB^+A}{A:\ H\text{–}B^+\text{–}H:A} \longrightarrow \underset{ABA^+}{A:\ H\text{–}B\ H\text{–}A^+} \qquad (3b)$$

$$\underset{A^+BA}{{}^+A\text{–}H\ B\text{–}H:A} \longrightarrow \underset{A^-B^-A^+}{{}^+A\text{–}H\ B:^-\ H\text{–}A^+} \qquad (4a)$$

$$\underset{A^+B^-A^+}{{}^+A\text{–}H\ B:^-\ H\text{–}A^+} \longrightarrow \underset{ABA^+}{A:\ H\text{–}B\ H\text{–}A^+} \qquad (4b)$$

(8) J. A. Pople and D. L. Beveridge, "Approximate Molecular Orbital Theory," McGraw-Hill, New York, N. Y., 1970.
(9) M. DePaz, S. Ehrenson, and L. Friedman, *J. Chem. Phys.*, **52**, 3362 (1970).
(10) As discussed by Pople and Beveridge,[8] geometric studies carried out with either CNDO/2 or INDO on closed-shell systems give essentially the same results.
(11) P. L. M. Plummer, *Bull. Amer. Phys. Soc., Ser. II*, **18**, 787 (1973).
(12) M. D. Newton and S. Ehrenson, *J. Amer. Chem. Soc.*, **93**, 4971 (1971).
(13) P. A. Kollman and L. C. Allen, *Chem. Rev.*, 72, 283 (1972).
(14) O. Tapia, A. Nogales, and P. Campano, *Chem. Phys. Lett.*, 24, 401 (1974).
(15) T. R. Singh and J. L. Wood, *J. Chem. Phys.*, **48**, 4567 (1968).
(16) R. Janoschek, E. G. Weidemann, and G. Zundel, *J. Chem. Soc., Faraday Trans. 2*, **69**, 505 (1973).
(17) J. L. Wood, *J. Mol. Struct.*, 17, 307 (1973).
(18) The "external" forces are those of protein structure and substrate or transition state binding in enzymic reactions and the covalent bonding forces of the molecular framework in intramolecular reactions.
(19) Adiabatic refers to the fact that the quantum state of the electrons of the system remains unchanged over the entire potential energy surface. See, for example, K. J. Laidler, "Theories of Chemical Reaction Rates," McGraw-Hill, New York, N. Y., 1969.
(20) M. Born and J. R. Oppenheimer, *Ann. Phys. (Leipzig)*, **84**, 457 (1927).
(21) M. Born and K. Huang, "Dynamical Theory of Crystal Lattices," Oxford University Press, New York, N. Y., 1954.
(22) R. Rein and F. Harris, *J. Chem. Phys.*, **43**, 4415 (1965).
(23) R. Rein and F. Harris, *J. Chem. Phys.*, **45**, 1797 (1966).
(24) S. Lunell and G. Sperber, *J. Chem. Phys.*, **46**, 2119 (1967).
(25) R. Janoschek, *Theor. Chim. Acta*, **32**, 49 (1973).

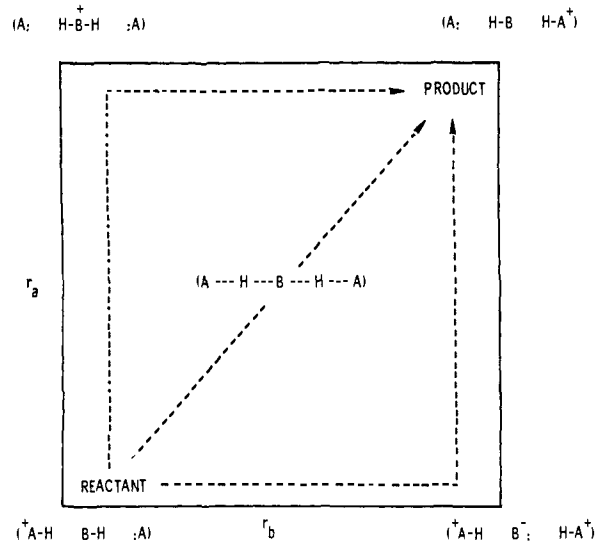

Figure 1. Key for interpreting contour maps (Figures 7–9). The cationic intermediate is located at the upper left-hand corner and the anionic intermediate at the lower right-hand corner. The dashed line through the center represents the dynamically coupled pathway, while the dashed lines through the cationic and anionic intermediates represent uncoupled cationic and anionic pathways, respectively. Further discussion can be found in the Terminology and Notation section.

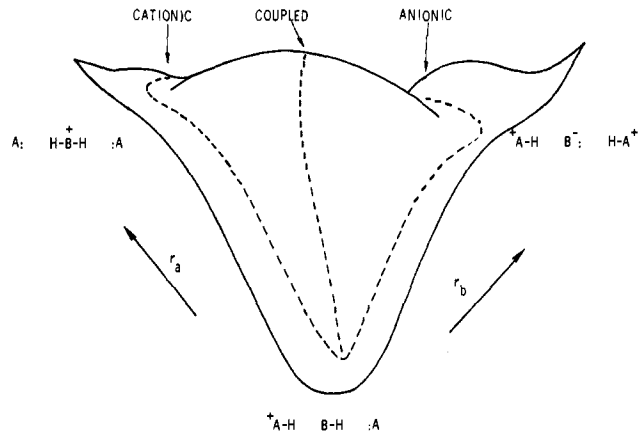

Figure 2. Key for interpreting transect diagrams (Figures 10–12). Dashed lines represent various pathways. The surface is viewed from the reactant (lower left) corner of the contour map in Figure 1. Further discussion of the nomenclature used can be found in the Terminology and Notation section.

For general reference, the *systems* are designated by the code for their reactant structure. Calculations were made for three different choices of the overall distance between proton donor and proton acceptor in each system. These are referred to as the "long" (A–B distance $\sim$ 3 Å), "medium" (A–B $\sim$ 2.75 Å), and "short" (A–B $\sim$ 2.5 Å) systems.

Graphical Representation of Potential-Energy Surfaces. For a given choice of the A–B distance R and of molecular identity for the AH, BH, and A species, the potential-energy surface can be generated by calculating the total energy of the system as a function of r_a and r_b (see eq 1). Since these two quantities are independently varied, we obtain a total energy corresponding to each pair of values, *i.e.*, $E = E(r_a,r_b)$. The potential-energy function $E(r_a,r_b)$ can then be represented as a three-dimensional potential-energy surface.

One such representation is the two-dimensional, energy contour map of Figure 1. Here r_a and r_b are taken as ordinate and abscissa, and contour lines of constant energy are plotted. The "reactant" species A^+BA and "product" species ABA^+ appear at the lower left and upper right corners, respectively. The "cationic intermediate" AB^+A and the "anionic intermediate" $A^+B^-A^+$ are then in the upper left and lower right corners, respectively.

Because the geometrical positions of A, B, and A are all fixed in the calculation (and in the physical situation, for example, an enzyme active site, which it may model), the surface thus generated is a dynamical surface: trajectories along the potential surface correspond to actual motions of the system proceeding from one structure to another. We can therefore identify the three reaction routes on the surface. The coupled pathway (eq 2) is shown by the diagonal dashed line of Figure 1, along which both r_a and r_b simultaneously change. The cationic pathway and the anionic pathway are the upper and lower bent, dashed lines, respectively. The exact shape of a given pathway will, of course, vary from system to system.

A different and frequently more visually satisfying version of the surface is the *transect diagram* of Figure 2. This simply projects the information of the contour map into three dimensions.

Hydrogen-Bond Potential Functions. Building-Up Principle. A profile through the potential-energy surfaces of Figures 1 and 2, taken parallel to either r_a or r_b, is a one-dimensional, hydrogen-bond potential function (the profile along r_a gives the function for the ^+A-H$\cdots$BH hydrogen bond in the presence of A; that along r_b corresponds to the BH$\cdots$A system in the presence of $^+$AH). Indeed, the entire surface can be envisioned as a manifold of such functions, exhibiting how the $^+$AH$\cdots$BH potential changes as the proton is removed from B or, alternatively, how the BH$\cdots$A potential changes as another proton is added to B. This semantic technique (discussing the character of the surfaces in terms of building-up from hydrogen-bond potentials) is enormously convenient and will be used below. To facilitate still further a development of the underlying physical picture, it is useful to consider how hydrogen-bond (X-H$\cdots$Y) potential functions, in general, are built up from their component (X–H and Y–H) bond-potential functions.

A number of theoretical investigations of the factors[26] which contribute to hydrogen-bond formation have been carried out.[27] In the present analysis, we employ a slightly different partition than is usually used but which is more convenient for our purposes.

(26) As pointed out by Coulson (see ref 27a, p 339), the resolution of the various factors contributing to the stability of a hydrogen bond, such as electrostatic interactions, delocalization effects, repulsive forces, and dispersion forces, is always somewhat arbitrary. Kollman and Allen[13] also provide a discussion of various "decomposition schemes" used, as well as a table (Table VI, ref 13) of the values obtained for a number of systems. It should also be pointed out that the present INDO calculations do not account for the dispersion contribution to the hydrogen bond energy since such a contribution depends on correlation effects, which are not obtainable for self-consistent field calculations. The dispersion energy for a "typical" hydrogen bond is $\sim$1.5 kcal/mol (ref 13).

(27) For general reference, see (a) "Hydrogen Bonding," D. Hadzi, Ed., Pergamon Press, Oxford, 1959; (b) S. Bratoz, *Advan. Quantum Chem.*, 3, 209 (1967); and (c) S. H. Lin, "Physical Chemistry: An Advanced Treatise," Vol. 5, H. Eyring, Ed., Academic Press, New York, N. Y., 1970, p 439.

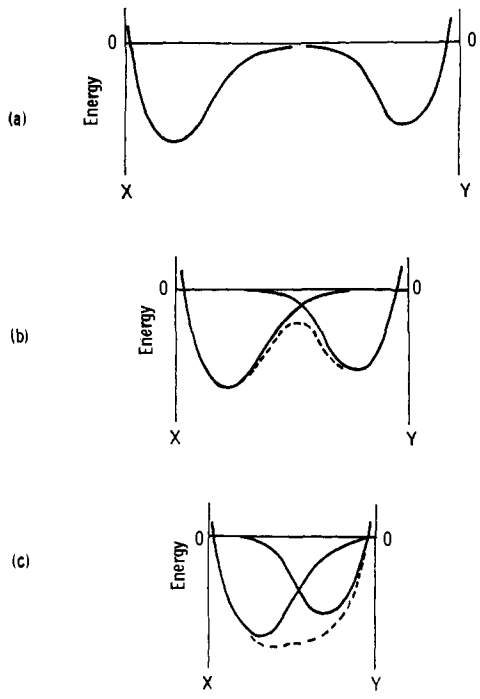

Figure 3. Illustration of the effect of internuclear separation on the formation of a double-welled potential function from two "isolated" component single-welled potential functions, E_{XH} and E_{YH}. The dotted lines indicate the sum of the two curves in regions where the sum differs from the component curves. Further discussion can be found in the Hydrogen-Bond Potential Functions section.

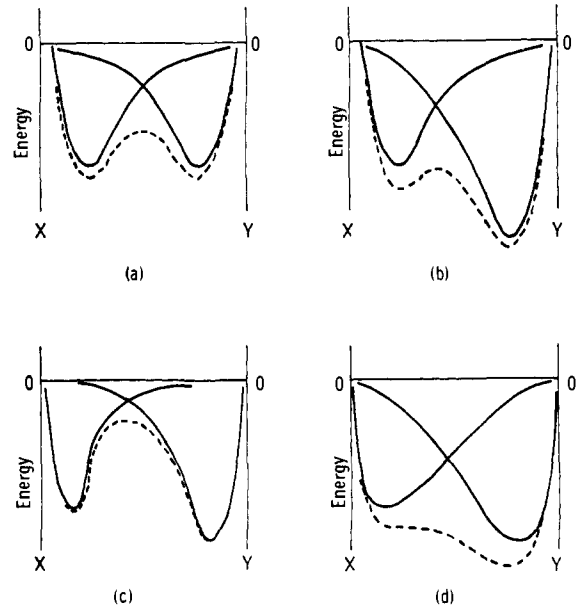

Figure 4. Illustration of the effects of relative well-depth and shape on the formation of double-welled potential functions from two "isolated" component single-welled potential functions, E_{XH} and E_{YH}. (a) and (b) represent the effect of increasing the well-depth of one of the component potentials. Both the equilibrium positions and the quadratic force constants were held constant so that the "shapes" of the component potentials were unchanged near their *equilibrium* positions. (c) and (d) represent the effect of changing the shapes of the component potentials. Both the equilibrium positions and well-depths of the component potentials were held constant. Further discussion can be found in the Hydrogen-Bond Potential Functions section.

Consider the potential function of the system X-H···Y (energy as a function of XH distance for a constant XY separation). In Figure 3a, the formation of the hydrogen-bond potential function from the two-bond potential functions is shown for a very large XY separation. Here the XH bond is completely broken before YH begins to form, and the barrier thus corresponds to the bond energies of XH or YH.

If a smaller separation of X and Y is considered as in Figure 3b, the simple superposition of the two-component potentials again generates a double-well function but now with a smaller barrier. The simultaneous interaction of the proton with X and Y, when it is at the center of the bond, lowers its energy there. Finally, at sufficiently short XY distances, as seen in Figure 3c, the hydrogen-bond potential collapses to a single-well function. This occurs when the favorable, simultaneous interaction with X and Y of the centrally located proton becomes dominant, yielding a "supermolecule" XHY.

A more careful treatment would include other terms beyond the superposition, as shown in eq 5, where

$$E_{XHY}(R,r) \cong E_{XH}(r) + E_{YH}(r) + E_{XY}(R) + \Delta E_{XH(Y)}(R,r) + \Delta E_{YH(X)}(R,r) + \Delta E_{XY(H)}(R,r) \quad (5)$$

E_{XH} and E_{YH} represent the potential-energy functions for isolated or unperturbed XH and YH molecules, respectively; E_{XY} represents the potential-energy function between X and Y, in the absence of a proton, which for a given, fixed intermolecular distance is a constant. The R and r coordinates (see eq 1) represent intermolecular (XY) and proton–molecule (XH or YH) distances, respectively. $\Delta E_{XH(Y)}$ and $\Delta E_{YH(X)}$ represent correction terms to the E_{XH} and E_{YH} potential-energy functions due to the presence of the Y and X attractive centers, respectively. And finally, $\Delta E_{XY(H)}$ represents a correction to the E_{XY} term brought about by the presence of the proton. $\Delta E_{XY(H)}$ generally provides stabilization to the usually repulsive E_{XY} term. This particular resolution of the energy components has a great similarity to the empirical Lippincott–Schroeder hydrogen-bond, potential-energy function which has shown wide applicability to a number of hydrogen-bonded systems.[28,29]

At large distances, terms other than E_{XH} and E_{YH} should make little or no contribution to E_{XHY} (recall that E_{XY} is constant for a given R). At closer distances, however, the attractive $\Delta E_{XH(Y)}$, $\Delta E_{YH(X)}$, and $\Delta E_{XY(H)}$ terms will stabilize the system, broadening the wells and lowering the barrier. These terms have the effect of removing the double-well character at larger R than would occur if only the E_{XH} and E_{YH} terms were considered.

In the more general case of unsymmetrical, overlapping potential-energy functions (Figure 4), we will, for the purposes of this discussion, consider the effect

(28) E. R. Lippincott, J. N. Finch, and R. Schroeder, ref 27a, p 361, and references cited therein.

(29) Each of the terms in eq 5 contains, *in principle*, all the different types of contributions to the energy, such as the static and induction energies and also the nonadditive three-body and higher interactions. Furthermore, the division of the two terms, $\Delta E_{XH(Y)}$ and $\Delta E_{YH(X)}$, is arbitrary since, when the proton is closer to a particular attractive center, *e.g.*, X, the potential it sees is *primarily* that due to E_{XH} and $\Delta E_{XH(Y)}$. As the proton moves toward Y, it begins to be more strongly influenced by E_{YH} and $\Delta E_{YH(X)}$. Hence, the point at which $\Delta E_{XH(Y)}$ becomes small and $\Delta E_{YH(X)}$ becomes important is arbitrary. The two terms are separated for convenience of discussion only.

of only the E_{XH} and E_{YH} terms. Three rules of thumb are both obvious and useful.

(1) For a constant XY separation and shape of E_{XH} and E_{YH}, the greater the difference in depth of the two wells, the lower will be the barrier (Figures 4a and 4b).

(2) For a constant difference in depth of well and XY separation, the shallower the contributing function, the lower will be the barrier (Figures 4c and 4d).

(3) For a constant XY separation, the minimum point of the single-well potential lies closer to the minimum point of the lower energy component function (Figures 3c and 4d).

The application of these rules to our potential-energy surface arises from the fact that four "coordinates" of interest form hydrogen-bond potentials in profile. Two of these represent the essentially uncoupled proton motions described approximately by r_a and r_b, for the hydrogen bonds corresponding to AH···BH and BH···A, respectively. The other two represent essentially symmetric and antisymmetric coupled proton motions. The symmetric motion along the cation–anion diagonal converts the cationic to the anionic intermediate. The potential can be thought of as a "double-hydrogen-bond" potential with the component-bond potentials (corresponding to E_{XH} and E_{YH}) being those for the processes $BH_2^+ \rightarrow B^- + 2H^+$ and $2AH^+ \rightarrow 2A + 2H^+$. The antisymmetric coupled motion converts reactants directly to products along the reactant–product diagonal. In this case, both component-bond potentials are approximated by the same potential function, that for $AH^+ + BH \rightarrow A + B^- + 2H^+$.

In the discussion of our potential surfaces, we will analyze the three-dimensional potential-energy surfaces in terms of such approximate hydrogen-bond potentials and their behavior.

Types of Proton-Transfer Processes. In the section on Terminology and Notation, we distinguished the anionic and cationic pathways of Figure 1, from the coupled pathway through the center. The implication was that the anionic and cationic pathways would pass through two activated complexes each, one for the formation and one for the decomposition of the intermediate. Each activated complex would involve the motion of only one proton (*e.g.*, the transition state for formation of AB^+A would be {A···H···B–H A}, while that for its decomposition would be {A H–B··· H···A}). Thus, these pathways would represent truly uncoupled motion.

In reality, the situation may be more complicated (Figure 5). For example, there could be a reaction pathway like that of Figure 5a, in which the system traverses only a single activated complex (at the black dot), but in which most of the overall route is parallel to one or the other of the axes. The general character of the pathway, or the *dynamics*, is thus "uncoupled." On the other hand, the reaction coordinate of such an activated complex (double-headed arrow) may well correspond to coupled motion, as shown. Any solution-kinetics experiment, within the confines of transition-state theory, will therefore decide that the reaction is coupled. Thus the measurable, *kinetic* character of the pathway is "coupled." We now distinguish *kinetic coupling* (reaction coordinate of the main activated complex involves coupled motion) and *dynamic coupling* (major part of entire reaction path involves coupled motion). The example of Figure 5a illustrates a dynamically uncoupled, kinetically coupled reaction. In Figure 5b, we see an alternative possibility. This pathway lies generally along the reactant–product diagonal (thus *dynamically coupled*), but in each of the two activated complexes, the reaction coordinate (double-headed arrows) involves the motion of only one proton (thus *kinetically uncoupled*).[30] Obviously, a reaction path can be both dynamically and kinetically coupled or uncoupled.[31]

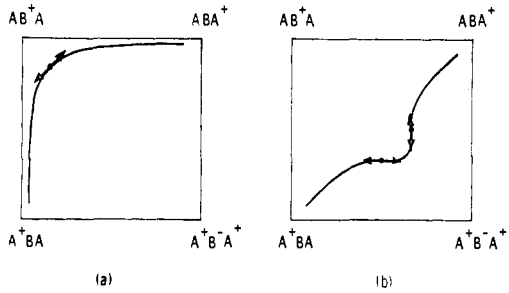

Figure 5. Schematic representations of (a) dynamically uncoupled, kinetically coupled, and (b) dynamically coupled, kinetically uncoupled pathways on the energy contour maps. Activated-complex locations are represented by heavy dots and reaction coordinates by double-headed arrows. Further discussion can be found in the Types of Proton Transfer Processes section.

The proton-transfer processes described so far are those which take place *over* potential-energy barriers, although proton tunneling through such barriers has also

(30) Pathways along which two successive and similar activated complexes occur deserve a special notice. Under circumstances where the intermediate species between these two complexes is very unstable and both activated complexes resemble each other strongly, *and* are of similar energy, the concept of rate-determining step becomes hazy. The free energy of activation observed in such a situation is given by eq i, where G_1^* and G_2^* are the free energies of the first and second acti-

$$\Delta G_0^* = RT \ln \{e^{G_1^*/RT} + e^{G_2^*/RT}\} - G_r \qquad \text{(i)}$$

vated complexes, and G_r is the free energy of the reactants. Any experiment which alters ΔG_0^*, represented by the operator δ_x, then produces an effect $\delta_x \Delta G_0^*$ given by eq ii, where f_2 and f_{-1} are the fractions of

$$\delta_x \Delta G_0^* = f_2 \delta_x G_1^* + f_{-1} \delta_x G_2^* - \delta_x G_r \qquad \text{(ii)}$$

intermediate species which proceed on to products and revert back to reactants, respectively. It is assumed that f_2 and f_{-1} are nearly unaltered by the experiment: R. L. Schowen and K. S. Latham, Jr., *J. Amer. Chem. Soc.*, **89**, 4677 (1967). Equation ii shows that the result of the experiment, $\delta_x \Delta G_0^*$, reflects a weighted average of the effects on the first activated complex, $\delta_x G_1^*$, and on the second activated complex, $\delta_x G_2^*$. If the experimenter is unaware that two activated complexes are indeed involved, he may determine an activated complex structure from a series of experiments, which is a weighted-average structure for the two activated complexes or the structure of a *virtual activated complex*. Note that the virtual activated complex for the path of Figure 5b, combining the two uncoupled motions with equal weight, would appear to be an activated complex for coupled motion, by most experimental criteria. Nevertheless, certain ingenious isotope-effect experiments are, in principle, capable of distinguishing the truly coupled case from that of Figure 5b: E. K. Thornton and E. R. Thornton in "Isotope Effects in Chemical Reactions," C. J. Collins and N. S. Bowman, Ed., Van Nostrand-Reinhold, New York, N. Y., 1970, pp 274–275. The arguments given here refer to free energy, while the calculations, of course, yield potential energies. For typical kinetic approaches to activated-complex structure in solution, it is likely that enthalpy–entropy compensation leads to potential-energy-based conclusions: R. L. Schowen, *J. Pharm. Sci.*, **56**, 931 (1967).

(31) The current common usage which corresponds most closely to our terms, coupled and uncoupled, is "concerted and stepwise." These terms have frequently been used with various meanings by various groups, however, and we shall avoid them in this paper to save confusion. It seems highly desirable for those using these terms to provide or refer to a definition of them corresponding to their intended meaning.

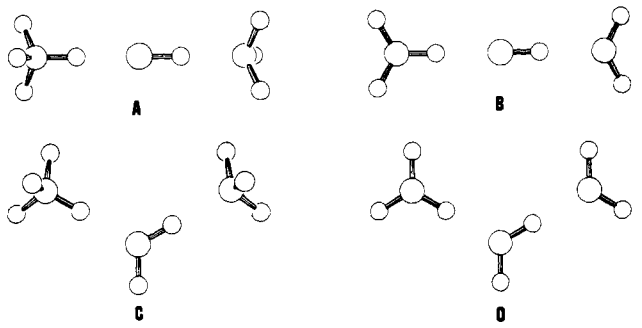

Figure 6. Scale drawings,[38] showing bond lengths and angles, for medium reactant (A^+BA) structures. Structure A is $H_3NH^+\cdots FH\cdots NH_3$, structure B is $H_2OH^+\cdots FH\cdots OH_2$, structure C is $H_3NH^+\cdots OH_2\cdots NH_3$, and structure D is $H_2OH^+\cdots OH_2\cdots OH_2$. Complete information on coordinates is given in Table I and discussed in the Experimental Section.

been discussed by a number of authors.[22-24,32-37] However, the experimental evidence currently available favors proton tunneling only in a very limited number of solution reactions of the type considered here.[37] We shall therefore assume that the most rapid reactions are those that traverse the lowest energy barriers.

Experimental Section

Procedure. The present calculations were carried out using the INDO method.[8] The basic computer program used in the calculations was obtained from the Quantum Chemistry Program Exchange at Indiana University (QCPE 141). The program was suitably modified to handle up to 150 basis functions, and matrix diagonalization was performed using a modified Givens algorithm also available through the Quantum Chemistry Program Exchange (QCPE 62.3). All computations were performed on the Honeywell 635 computer at the University of Kansas Computation Center. The computational time for each point used in the construction of a surface was approximately 0.025 hr.

The geometries of the systems were determined from the following considerations. The transfer of the protons should occur linearly, *i.e.*, at an A–H–B angle of 180°. The structures of H_3O^+ and H_2O contained H–O–H angles of 117.90° and O–H distances of 1.046 Å for the nontransferring protons. The structures of NH_4^+ and NH_3 contained H–N–H angles of 109.47° and N–H distances of 1.079 Å for the nontransferring protons. These angles and distances were determined by minimization of the energy of H_3O^+ and NH_4^+ by the INDO method, and the same distances and angles were adopted for the H_2O and NH_3 moieties which become protonated during the reaction. A linear structure for HFH^+ was assumed, and minimization of the energy occurred at an H–F bond distance of 1.035 Å. The systems used are illustrated in the ORTEP[38] drawings of Figure 6, and the coordinates for each are given in Table I. These geometries have little effect on the qualitative shape of the surface, as determined by additional calculations on the same systems using experimental bond angles and distances.

The potential-energy surfaces were constructed with the bond distances, r_a and r_b, as two of the axes and the total energy as the third axis. Table II presents a summary of the values of the r_a, r_b, and the A–B distance R for the surfaces reported.

Each coordinate was divided into ten equally spaced increments so that, including the extremes, 11 points were computed for both r_A and r_B. This generates a matrix of 121 points. Since the potential-energy surfaces are symmetric about the cation–anion diagonal, only 66 points were calculated for each surface, with the remaining points being obtained by reflection about the diagonal. The lowest calculated, total-energy point on a given surface was assigned an energy of 0 kcal/mol, and the energies of the remaining points were calculated relative to it. These data were then plotted by surface II[39] to give the contour maps and transect diagrams shown. The heavy-atom distances R were chosen to represent reasonable distances for hydrogen-bonded systems of this type.[13]

Table I. Coordinates for Systems A, B, C, and D in Figure 6 (in Ångströms)

Atom	X	Y	Z
	A = $NH_4^+\cdots FH\cdots NH_3$		
F	0.0	0.0	0.0
N	2.720000	0.0	0.0
N	−2.720000	0.0	0.0
H	−3.079667	−0.881000	−0.508645
H	−3.079667	0.0	1.017291
H	−3.079667	0.881000	−0.508645
H	3.079667	−0.881000	0.508645
H	3.079667	0.0	−1.017291
H	3.079667	0.881000	0.508645
H	1.080000	0.0	0.0
H	−1.640000	0.0	0.0
	B = $H_3O^+\cdots FH\cdots H_2O$		
F	0.0	0.0	0.0
O	−2.750000	0.0	0.0
O	2.750000	0.0	0.0
H	−3.239455	−0.896127	0.226953
H	−3.239455	0.896127	0.226953
H	3.239455	−0.896127	−0.226953
H	3.239455	0.896127	−0.226953
H	1.040000	0.0	0.0
H	−1.710000	0.0	0.0
	C = $NH_4^+\cdots H_2O\cdots NH_3$		
O	0.0	0.0	0.0
N	2.33027	1.345383	0.397717
N	−2.33027	1.345383	0.397717
H	0.0	−1.034758	0.152946
H	2.509585	1.448910	1.456664
H	−2.509585	1.448910	1.456664
H	2.262314	2.323439	−0.052872
H	−2.262314	2.323439	−0.052872
H	3.143314	0.797502	−0.052872
H	−3.143314	0.797502	−0.052872
H	0.865285	0.499572	0.147682
H	−1.464987	0.845811	0.250035
	D = $H_3O^+\cdots H_2O\cdots H_2O$		
O	0.0	0.0	0.0
O	2.355973	1.360222	0.402104
O	−2.355973	1.360222	0.402104
H	0.0	−1.034758	0.152946
H	2.355973	2.394980	0.249158
H	3.252100	0.842843	0.249158
H	−3.252100	0.842843	0.249158
H	−2.355973	2.394980	0.249158
H	−1.464987	0.845811	0.250035
H	0.865285	0.499572	0.147682

Results and Discussion

General Survey of the Surfaces. The results are portrayed in Figures 7–9 (contour maps) and 10–12 (transect diagrams). Each figure contains surfaces for a single choice of "heavy-atom" distance (see Table II), so that Figures 7 and 10 give the results for the long systems, 8 and 11 those for medium systems, and 9 and 12 those for short systems. Each figure has four diagrams, one for each of the N^+FN, O^+FO, N^+ON, and O^+OO systems. The top row of the diagrams consists

(32) P. O. Löwdin, *Advan. Quantum Chem.*, 2, 213 (1965).
(33) J. J. Weiss, *J. Chem. Phys.*, 42, 1120 (1964).
(34) E. F. Caldin and M. Kasparian, *Discuss. Faraday Soc.*, **39**, 25 (1965).
(35) H. J. Gold, *Acta Biotheor.*, 20, 29 (1971).
(36) M. D. Harmony, *Chem. Soc. Rev.*, 1, 211 (1972); *cf.* H. S. Johnston, "Gas Phase Reaction Rate Theory," Ronald Press, New York, N. Y., 1966, p 190 et passim.
(37) E. S. Lewis, private communication.
(38) C. K. Johnson, ORTEP-II, ORNL-3794, Oak Ridge National Laboratory, Oak Ridge, Tenn.
(39) R. J. Sampson, "Users' Manual for the Surface II Graphics System," Tech. Report, KOX. Project, Kansas Geological Survey, Lawrence, Kan., 1973. The experimentally determined matrix of 121 points was converted into a new matrix of 625 points by a linear least-squares interpolation. Smoothing routines were used in connecting these points for construction of the contour maps and transect diagrams.

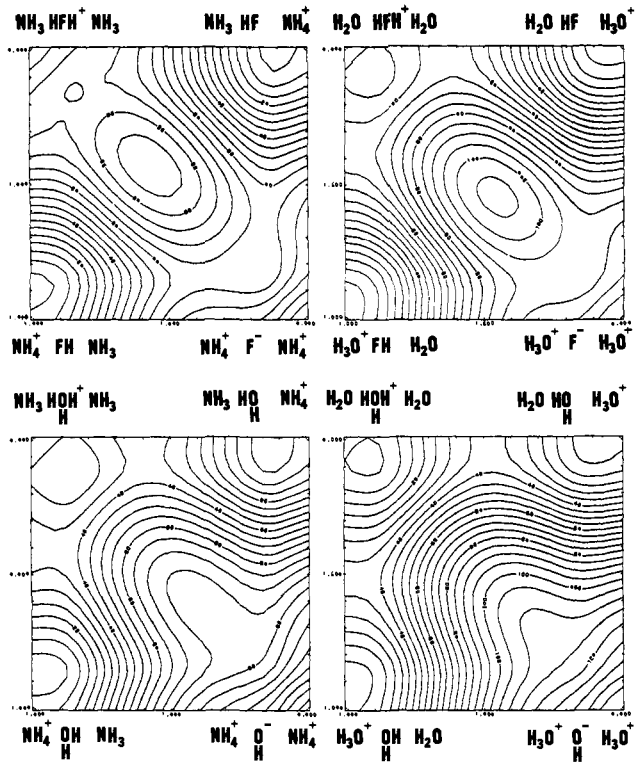

Figure 7. Contour maps (resolution 5 kcal/mol) for the potential-energy surfaces of long systems. The vertical axis is r_a, the horizontal axis is r_b, and the distances shown are in Å (*cf.* Figure 1). The anionic intermediates for the N^+FN and the O^+FO systems are at potential minima, as shown by higher resolution surfaces, although it is not obvious from these maps. The species $N^+F^-N^+$ is isolated by barriers of at least 3 kcal/mol. The species $O^+F^-O^+$ is isolated by barriers of at least 2 kcal/mol.

Table II. Heavy-Atom Distances and Coordinates for Surfaces (in Ångströms)

A–H	B–H		Long	Medium	Short
		R	3.00	2.72	2.48
$^+NH_4$	OH_2	$r_a = r_b$	1.00–2.00	1.01–1.71	1.04–1.44
		R	3.00	2.72	2.48
$^+NH_4$	FH	$r_a = r_b$	1.00–2.00	1.01–1.71	1.04–1.44
		R	3.00	2.75	2.50
H_3O^+	OH_2	$r_a = r_b$	1.00–2.00	1.025–1.725	1.00–1.50
		R	3.00	2.75	2.50
H_3O^+	FH	$r_a = r_b$	1.00–2.00	1.025–1.725	1.00–1.50

of the N^+FN and O^+FO surfaces, and the bottom row the N^+ON and O^+OO surfaces. Thus, each row has a constant bridging structure (HF in the top row, H_2O in the bottom row) and different donor–acceptor structures (NH_3 in the left surface, H_2O in the right surface). To see how increased acidity–decreased basicity in the donor–acceptor structure affects the surface, one therefore glances from left to right in each figure. Similarly, the left column in each figure always has H_2O as the donor–acceptor, while the right column always has NH_3 as the donor–acceptor. Glancing from top to bottom of each column, one sees the effect of decreased acidity–increased basicity as the bridging structure changes from HF to H_2O with constant donor–acceptor.[40]

(40) Due caution should be exercised in the use of the concepts of "acidity" and "basicity," because (a) these qualities differ in the gas and liquid phases, and (b) effects on neighboring structures may alter the effective acidity or basicity of a species from that expected for it in isolation. In the above cases, the notions of acidity and basicity are meant to be used only qualitatively.

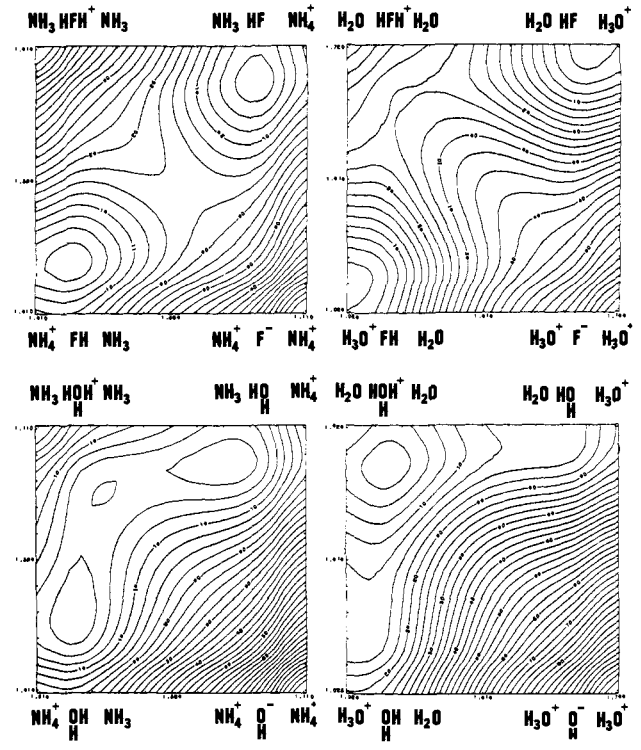

Figure 8. Contour maps (resolution 2.5 kcal/mol) for the potential-energy surfaces of medium systems. The vertical axis is r_a, the horizontal axis is r_b, and the distances shown are in Å (*cf.* Figure 1).

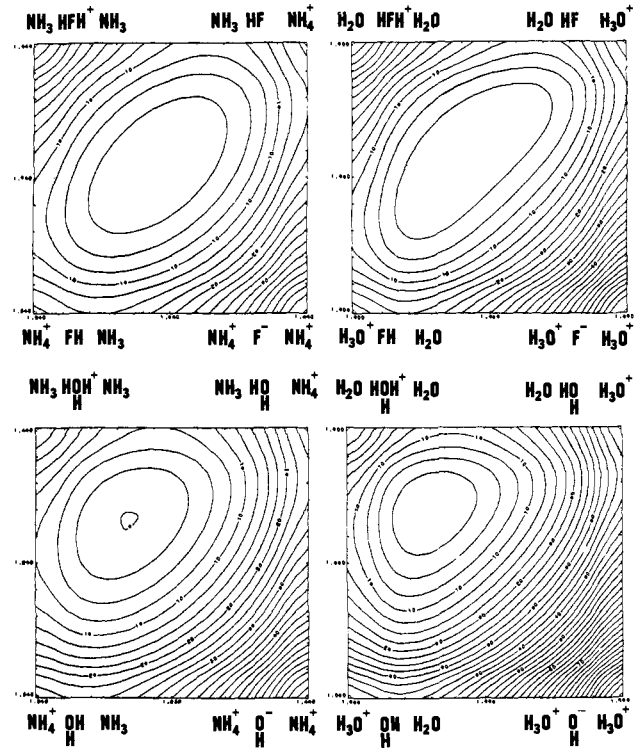

Figure 9. Contour maps (resolution 2.5 kcal/mol) for the potential energy surfaces of short systems. The vertical axis is r_a, the horizontal axis is r_b, and the distances shown are in Å (*cf.* Figure 1).

First, we examine the general effect of changing the "heavy-atom" distance. From Figures 7 and 10, the long systems all clearly produce *double-well surfaces*, in that the energy profile along each edge of the surface is a double-well potential. Reactants, products, cationic

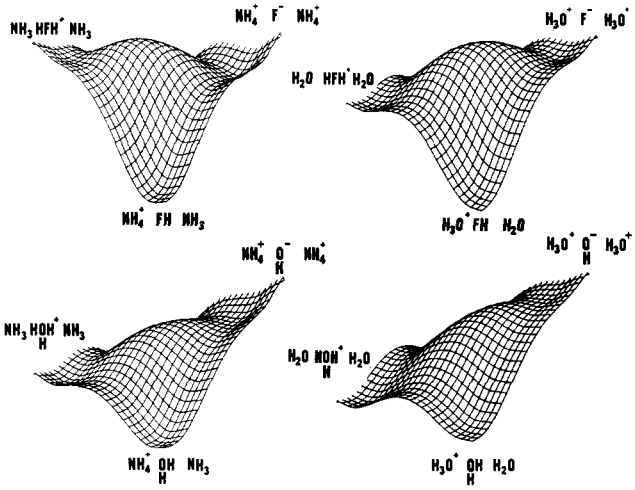

Figure 10. Transect diagrams of the potential-energy surfaces for long systems. Each side of the surfaces is 1 Å in length. The viewpoint for these surfaces is defined relative to the center of the basal r_a, r_b plane of the contour maps (Figure 7), which includes the lowest energy point on each surface. The viewing point is located a distance of 4 Å from the center of the r_a, r_b plane on a line 22.5° above the plane and 5° clockwise toward the cationic intermediate from the reactant-product diagonal. The distance in energy between the reactant structure and the high central point is approximately 85 (N^+FN), 105 (O^+FO), 75 (N^+ON), and 100 kcal/mol (O^+OO).

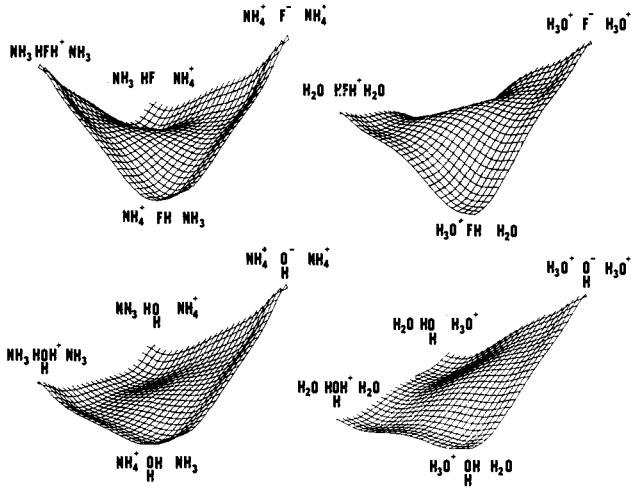

Figure 11. Transect diagrams of the potential surfaces for medium systems. Each side of the surfaces is 0.7 Å in length. The viewpoint here is the same as that in Figure 10, except that the location of the observation point is only 2.8 Å from the center of the basal plane. The distance in energy from the reactant structure to the center point of the surface is approximately 17 (N^+FN), 35 (O^+FO), 15 (N^+ON), and 20 kcal/mol (O^+OO).

and anionic intermediates are all definite species at minima on the potential surface (a fact which is more obvious from the transect diagrams than from the contour maps). The reactant–product diagonal and cation–anion diagonal are also double-well potentials. At this separation of the heavy atoms, therefore, the system exhibits double-well character in all forms of proton motion. Presumably, the distance to be traversed in *any* proton-transfer process is sufficient that the proton finds itself at an energy maximum at some point along the way.

The short systems of Figures 9 and 12, on the other hand, give surfaces which are strictly *single-well surfaces*. Along each edge and along both diagonals, a single minimum is seen. Apparently the component bond potentials at these small heavy-atom separations overlap so strongly that the proton always finds it advantageous to remain at some intermediate position between its two neighbors. Indeed, the stablest arrangement is one in which both protons are simultaneously at intermediate positions, giving the "supermolecule" with a structure somewhere toward the center of the potential surface. The structure of the "supermolecule" can be described as a resonance hybrid of the reactant, product, anionic and cationic intermediate structures[41] and will lie closest to the most stable of these species.

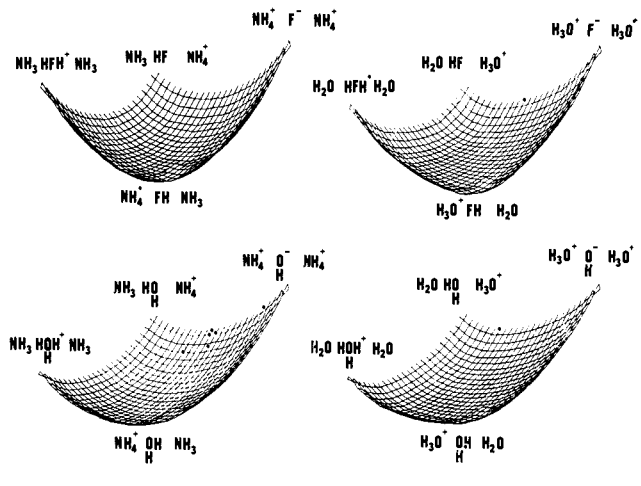

Figure 12. Transect diagrams of the potential surfaces for short systems. Each side of the N^+FN and N^+ON surfaces is 0.4 Å in length, while each side of the O^+FO and O^+OO surfaces is 0.5 Å in length. The viewpoints for these diagrams are the same as that of Figure 10, except that the observation point is 1.6 Å for the N^+FN and N^+ON surfaces, and 2.0 Å for the O^+FO and O^+OO surfaces, from the center of the basal plane. The distance in energy from the lowest point of the surface to the highest point (the anionic corner in all cases) is 45 (N^+FN), 65 (O^+FO), 68 (N^+ON), and 100 kcal/mol (O^+OO).

The medium systems, seen in Figures 8 and 11, fall appropriately between the extremes in their behavior and exhibit a greater diversity than either the long or short systems. The barriers along the edges of the diagrams are only of the mildest sort. The potential minima corresponding to the various species (particularly the cationic and anionic intermediates) are very shallow and consist of depressions on the surfaces, which are only just visible in the transect diagrams of Figure 11. While the reactant–product diagonal remains double-welled in all cases, the cation–anion diagonal has degenerated to essentially a single-well potential.

These results are just those anticipated from the hydrogen-bond building-up principle. Long systems should give double-well potentials, short systems single-well potentials, and medium systems something in between. The interesting finding is that these predictions, which are straightforward for the simple profiles taken along the edges (single-proton, uncoupled motions), extend also to the coupled motions along the diagonals of the potential surface. Long systems, with highly defined species at all four corners of the surface

(41) (a) M. Ettlinger and E. S. Lewis, *Tex. J. Sci.*, **14**, 58 (1962); (b) *cf.* J. E. Leffler, *Science*, **117**, 340 (1953).

and energy maxima along each edge, generate a still higher maximum in the center of the surface, where the maxima along the two-diagonal coordinates tend to coincide. Short systems, with minima along each edge, generate a still deeper minimum at the center, where the minima for the two diagonals reinforce.

Consequences of the General Features. One practical mechanistic consequence of the features is this: where intermediate species are well-defined entities, with potential barriers separating them from reactants and products, the favored reaction pathways will be dynamically uncoupled, passing through the intermediates, with the point corresponding to the activated complex of the coupled route being an absolute potential maximum, rather than a saddle point. This means that proton transfers among groups linked by "normal" hydrogen bonds having double-well potentials will always follow an uncoupled route. Only under circumstances where a single-well potential prevails for one or more hydrogen bonds in the chain can a coupled process become important. This is to say that a coupled pathway is only possible if the intermediates have no actual existence as chemical species, not lying at relative minima on the potential surface.

A second practical consequence is that the mechanism of proton transfer in certain systems may be altered from uncoupled to coupled, merely by changing the distance between the end groups. This is illustrated by the N^+FN surfaces at long and medium distances. At the long distance, the pathway is uncoupled, but at the medium distance, the mechanism goes over to a coupled route. As can be seen in Figure 11, the route for the medium distance lies across the center of the diagram with the activated complex being slightly anionic of the center. The mechanism at this distance is thus dynamically and kinetically coupled. Therefore, it is possible for proton-transfer processes involving an identical array of functional groups to proceed by a coupled pathway in a molecular environment which compresses the groups, but by an uncoupled pathway in an environment which allows or constrains a greater separation among them. It seems likely that intermolecular proton transfers among an assembly of otherwise independent molecules, temporarily hydrogen-bonded, would most prefer an uncoupled mechanism since, other things being equal, the tendency to maintain relative long end-group distances should be strong. This situation corresponds to many model acid–base catalysis systems, in which, for example, a substrate, one or more water molecules, and a catalyzing acid or base are assembled for reaction. The hydrogen bonds among these reaction partners will naturally tend to be long and double-welled, yielding an uncoupled mechanism.[42] On the other hand, a greater tendency for coupled proton transfers should be observed in those intramolecular reactions in which some or all of the participating functions are held by covalent bonds in close proximity. In cases where this proximity is sufficient to produce single-well hydrogen bonds, the possibility of coupled proton transfer arises.

Most interesting of all is the situation in an enzyme active site. With an appropriate choice of functional-group array, possibly the famous carboxylate–imidazole–serine chain of the "charge-relay" system,[7] molecular evolution is capable of building either the coupled or uncoupled mechanism into a given enzymic system, simply by construction of the macromolecule so as to achieve the appropriate end-group separations. An enzyme with a "short" chain will tend to favor coupled proton transfer, while an enzyme with a "long" chain will tend to prefer the uncoupled process. Furthermore, the flexibility of protein structures and the sensitivity of the potential surfaces to changes in the end-group distances suggest that, for a single enzyme, a coupled mechanism might be observed with one substrate and an uncoupled mechanism with another substrate. This could occur if one substrate induced a "long" chain. Another possibility is that, for a given substrate and enzyme, allosteric effectors could shift the mechanism from coupled to uncoupled, or *vice versa*. This could be accomplished by the effector's binding at a remote site and inducing a protein conformation change, which would alter the structure at the active site from a "short" chain to a "long" chain, or *vice versa*.

Conditions for Dynamic Coupling. It may be inferred from the long and medium surfaces that an uncoupled mechanism (universal at long separations) cannot always be converted to a coupled mechanism merely by compression of the system to closer end-group distances. In fact, this occurs only for the N^+FN system, while the other three continue to exhibit dynamically uncoupled pathways even at the medium distance. Therefore, chemical conditions must also be appropriate for coupling to occur. The requisite condition is that the energies of the cationic and anionic intermediates not differ much. A large discrepancy in their energies forecloses the possibility of a path which is dynamically coupled.

This requirement emerges from the hydrogen-bond building-up principle applied to the cation–anion diagonal potential, in particular, from rule 3 given in the introductory section. If compression of the system is to convert an uncoupled mechanism to a dynamically coupled mechanism, then the energy maximum which dominates the central region of all long surfaces must diminish and be replaced by the saddle point of the coupled path as the end-group separation is shortened and the cation–anion diagonal becomes a single-minimum potential. But this emerging saddle point must not shift toward either the cationic or the anionic region as compression occurs; if it does, the mechanism will become a dynamically uncoupled one, whatever its kinetic character. As rule 3 shows, only if the cationic and anionic intermediates have nearly equal energies will the minimum point of their single-well potential lie near the midpoint of the cation–anion diagonal. If their energies are not equal, the single-well minimum and thus the reaction path will appear near the more stable of the intermediates, and the mechanism will be dynamically uncoupled. In fact, for the N^+FN system [$E(AB^+A) - E(A^+B^-A^+) = \Delta E \sim +16$ kcal/mol], the intermediates are of similar energy, and the mechanistic changeover occurs. For the O^+FO ($\Delta E \sim -38$ kcal/mol), N^+ON ($\Delta E \sim -56$ kcal/mol), and O^+OO ($\Delta E \sim -113$ kcal/mol) systems, the cationic intermediates are more stable than the anionic intermediates, and mechanistic routes are cationic and dynamically uncoupled at the medium separation.

(42) It is interesting that many recent calculations for hydrogen-bonded systems yield single-minimum potentials, with short end-group distances at the equilibrium geometry, so that this intuitive argument may be incorrect.[13]

Table III. Summary of Structural, Energetic, and Mechanistic Results[a]

System	ΔE°_{cat}	ΔE^*_{cat}	ΔE°_{an}	ΔE°_{an}	ΔE	Favored pathway	Coupling: Kinetic	Coupling: Dynamic
O^+OO long	−9	28	103	103[b]	−112	Cat.	No	No
N^+ON long	22	37	78	78[b]	−56	Cat.	No	No
O^+FO long[c]	52	67	90[c]	93	−38	Cat.	No	No
N^+FN long[c]	74	76	58[c]	63	+16	An.	No	No
O^+OO medium	Intermediates are too ill-defined to permit detailed evaluation of energetics					Cat.	No	No
N^+ON medium						Cat.	No	No
O^+FO medium						Cat.	Yes	No
N^+FN medium						~An.[d]	Yes	Yes
Short systems	All short systems show a single "supermolecule" minimum							

[a] Energy changes, given in kcal/mol, are defined as: $\Delta E^\circ_{cat} = E(AB^+A) - E(A^+BA)$; $\Delta E^*_{cat} = E$(activated complex of cationic pathway) $- E(A^+BA)$; $\Delta E^\circ_{an} = E(A^+B^-A^+) - E(A^+BA)$; $\Delta E^*_{an} = E$(activated complex of anionic pathway) $- E(A^+BA)$; $\Delta E = E(AB^+A) - E(A^+B^-A^+)$. [b] The anionic intermediate is represented by a plateau rather than a minimum. [c] Although the minima for the anionic intermediates on these surfaces cannot be clearly seen in Figure 7, they are obvious on the more detailed surfaces (1 kcal/mol resolution) from which these data were taken. [d] This pathway, as careful examination of Figure 8 will show, lies slightly to the anionic side.

Thus in general, for a dynamically coupled mechanism to arise, it must be true that the cationic and anionic intermediates not differ greatly in energy.

Conditions for Kinetic Coupling. In the long systems of Figures 7 and 10, the reaction paths are both dynammically and kinetically uncoupled. As we have just seen, compression of the system to the medium distance results in dynamic and kinetic coupling for the N^+FN system which has nearly isoenergetic intermediates. Two of the other systems, N^+ON and O^+OO, clearly maintain both dynamically and kinetically uncoupled paths, activated complexes appearing before and after the favored cationic intermediate in each case.

The O^+FO surface presents a contrast. Here the path is dynamically uncoupled and unambiguously cationic. However, the cationic intermediate itself is probably nonexistent, and the activated complexes, expected before and after it, appear to have coalesced into a single structure on the cation–anion diagonal. Thus the path is a kinetically coupled one, the reaction coordinate in the single activated complex being parallel to the reactant–product diagonal. The reason for kinetic coupling in the O^+FO system, while the N^+ON and O^+OO paths remain kinetically uncoupled, appears when the energy difference between reactant and cationic intermediate is examined.

This quantity (taken from the long surfaces) is 52 kcal/mol for the O^+FO system, 22 kcal/mol for N^+ON, and −9 kcal/mol for O^+OO. Thus kinetic coupling seems to arise for dynamically uncoupled systems, when the energy difference between reactant and favored intermediate becomes very large. That this result is general and rational emerges from rule 1 of the section on the hydrogen-bond building-up principle: when the energy difference in question is sufficient, there will be no barrier between reactant and intermediate. When this is so, the path along the route of this (now nonexistent) "intermediate" must become kinetically coupled.

Summary of Rules for Coupling. We can summarize our findings about the circumstances under which coupled and uncoupled mechanisms are permitted in the following way.

(1) At quite long end-group distances, all systems show only uncoupled mechanisms.

(2) As end-group distances become shorter, dynamic coupling *can* arise *if* the cationic and anionic intermediates are nearly isoenergetic.

(3) If the intermediates are nearly isoenergetic and one or both of the potentials linking the reactant and the intermediates become single-welled, a dynamically coupled, kinetically coupled mechanism will result. As long as these reactant–intermediate potentials are double-welled, the uncoupled paths will dominate.

(4) If the intermediates are distant in energy from one another, and if the reactant–intermediate potential for the favored intermediate is double-welled, the mechanism will be dynamically and kinetically uncoupled.

(5) The intermediates being relatively distant in energy, and if the reactant–intermediate potential for the favored intermediates has become single-welled, then the mechanism will be dynamically uncoupled but kinetically coupled.

These rules are confirmed and illustrated by the data shown in Table III.

The Brønsted Law and the Hammond Postulate. It follows directly from the hydrogen-bond building-up principle that a single-proton transfer reaction which is more exothermic will have (a) a lower activation energy and (b) an activated complex with a smaller degree of proton transfer.

To test whether the first of these rules is obeyed on the surfaces calculated here, we read ΔE°, the energy of reaction for any pathway, and ΔE^*, the energy of activation for that pathway, from each of the long surfaces. On the other surfaces, the lower resolution would make specification of the activated-complex structures less reliable. A plot of ΔE^* *vs.* ΔE° for both anionic and cationic pathways on the long surfaces is shown in Figure 13. It is roughly linear, with a slope around 0.8. This confirms that the Brønsted Law[43] is obeyed by these systems.

To test the second point, we traced out the cationic and anionic pathways on the long surfaces (*cf.* Figure

(43) The Brønsted catalysis law (J. E. Leffler and E. Grunwald, "Rates and Equilibria and Organic Reactions," Wiley, New York, N. Y., 1963, p 235) states that free energies of activation for proton-transfer reactions will be linearly related to the free energies of reaction. In recent times, it has been considered likely by many [*cf.* R. L. Schowen, *Progr. Phys. Org. Chem.*, 9, 275 (1972)] that the slope of this linear relation (the Brønsted coefficient) is a measure of the degree of proton transfer in the activated complex. The value of 0.8 for this slope probably results from the relative endothermicity of most of the pathways on this surface. Indeed, the point for the only exothermic process departs from the relation considerably. The high degree of proton transfer in endothermic processes is predicted by Hammond's postulate, which is considered in the next paragraph. A review of recent developments concerning the Brønsted relation has been provided by A. J. Kresge, *Chem. Soc. Rev.*, 2, 475 (1973).

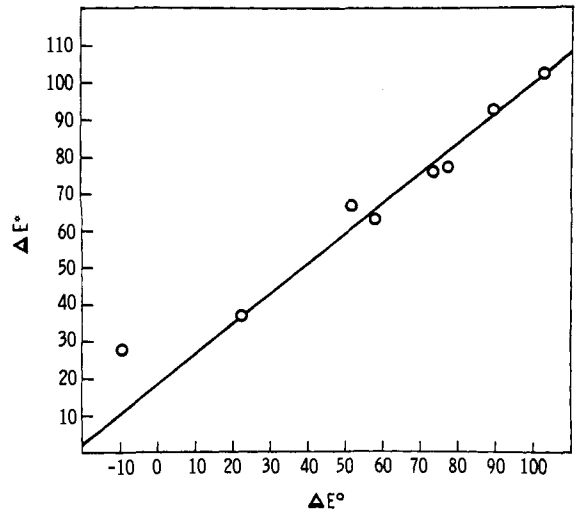

Figure 13. Plot of ΔE^*, the activation energy, *vs.* ΔE°, the energy of reaction, for various pathways on the long surfaces (data from Table III). All points for $\Delta E^\circ > 0$ fall roughly on a common line of slope ~0.8. Energies are in kcal/mol.

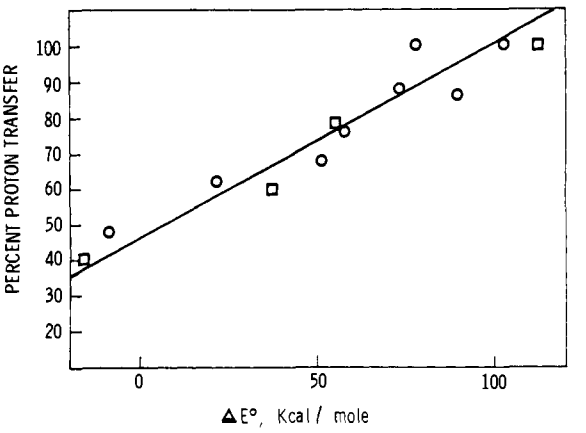

Figure 14. "Per cent proton transfer" as a function of ΔE° for various processes on the long surfaces. Circles refer to reactant–intermeidate potentials and squares to cation–anion potentials. As ΔE° increases, so does "per cent proton transfer," as discussed in the section on The Brønsted Law and the Hammond Postulate.

7) and located the activated-complex points, as before, on each. We then calculated the "per cent proton transfer" at the activated complex as the ratio of (distance between reactants and activated complex) to (distance between reactants and terminal point); both distances were measured directly on the surface. We made the same calculation for the cation–anion diagonal, even though the "activated complex" along this diagonal is actually an absolute maximum. A plot of "per cent proton transfer" *vs.* ΔE°, the energy of each reaction, is shown in Figure 14. Clearly, more endothermic reactions have higher "per cent proton transfer," as required by Hammond's postulate,[41b,44] and the relationship is roughly linear. In fact, the plot implies that a ΔE^* of about 100 kcal/mol is sufficient to produce a completely "product-like" activated complex (100% proton transfer), while, as expected, a ΔE^* of 0 yields 50% proton transfer.

Thus, the calculations fully confirm the applicability of both the Brønsted law and the Hammond postulate to the component proton-transfer processes. Further, both of these apply as well to the potential along the cation–anion diagonal, as they do to the conventional energy profiles along the edges. This means that, in general, it should be possible on a long surface, to locate all the activated complexes and the "hump" in the middle merely from a knowledge of the energies of reactants, products, and intermediates. It should be true (from the Brønsted law) that the favored reaction path (lower ΔE^*) will be that which passes through the lower energy intermediate (*i.e.*, low-energy intermediates are formed with low activation energy, and high-energy intermediates are formed with high activation energy). Thus, when one knows which intermediate is of lower energy, one knows that the pathway through that intermediate is the favored route. Furthermore, from Hammond's postulate, one can deduce that the activated complex(es) along the favored path will resemble either the intermediate or the reactant–product, whichever is more stable.

Comparison with Previous Work. The use of three-dimensional potential surfaces, or contour maps, to discuss coupling in multiple proton-transfer reactions seems to have originated with Albery.[45] Albery's treatment included other degrees of freedom, such as the librational motion of the participating structures, and his surfaces were derived completely by qualitative reasoning. It is therefore particularly noteworthy that he arrived at a surface which is qualitatively (and semiquantitatively) identical with our O⁻OO long system of Figures 7 and 10, for the transfer of a proton along a chain of water molecules. Albery also enunciated a principle which, as we shall see below, plays a considerable role in the construction and interpretation of these surfaces. Referring to the equivalent of our cation–anion diagonal, he noted that a triple-minimum potential function should be "*a priori*. . . unlikely." Clearly component single-minimum potentials can overlap to generate either a single-minimum or a double-minimum potential, but the sum can never have a third minimum.

Before Albery's work, concern with the theory of coupling in chemical processes had been centered on such reactions as nucleophilic substitution and β elimination. In nucleophilic substitution, a bond to the nucleophile is formed, and a bond to the leaving group is broken. These processes may be coupled (SN2 or "concerted displacement") or uncoupled, in which case the reaction path may pass through a cationic intermediate (a carbonium ion in SN1 displacement at carbon, when the leaving-group bond is cleaved before the nucleophile binds) or through an anionic intermediate (an adduct in which both nucleophile and leaving group are simultaneously bound to the center undergoing substitution.)[46] In β elimination, a bond to a proton and to a leaving group on an adjacent car-

(44) This principle, developed in mathematical form over a considerable period (see R. P. Bell, "The Proton in Chemistry," 2nd ed, Cornell University Press, Ithaca, N. Y., 1973, Chapter 10), was first given clear chemical substance by G. S. Hammond, *J. Amer. Chem. Soc.*, 77, 334 (1955).

(45) W. J. Albery, *Progr. React. Kinet.*, 4, 353 (1967).

(46) Although such adducts are unknown and unlikely in displacement at carbon, they occur in displacements at heavier centers such as silicon: L. H. Sonmer, "Stereochemistry, Mechanism and Silicon," McGraw-Hill, New York, N. Y., 1965). Indeed, both coupled and uncoupled displacements at silicon occur under similar conditions: C. G. Swain, K.-R. Pörschke, W. Ahmed, and R. L. Schowen, *J. Amer. Chem. Soc.*, 96, 4700 (1974)].

bon are both broken. The coupled process is known as E2 elimination, while passage through a cationic intermediate by prior uncoupled loss of the leaving group is denoted E1 elimination and passage through an anionic intermediate by prior uncoupled loss of the proton, E1cb elimination ("cb" means "conjugate base").

Attempts to extend Hammond's postulate in a very general way to these complex processes produced a certain amount of confusion. much of which was relieved by Thornton's elucidation[47] of the physical basis of the Swain–Thornton rule,[48] a generalization intended to supersede simple extensions of Hammond's postulate then current. In the context of the present calculations, Thornton's work had two striking effects. First, it focused attention on the necessity for approaching such problems as coupling through a detailed analysis of processes taking place in the activated complex. Second, it clarified the role of what we have called the cation–anion diagonal (Thornton's "perpendicular coordinate") as the main source of "anti-Hammond behavior."

The synthesis of these ideas into a potential-surface treatment of coupling which is directly ancestral to the present one was stimulated by an experimental observation of More O'Ferrall, who collected data which indicated that 9-fluorenylmethanol was undergoing *simultaneous* E2 and E1cb elimination. This was contrary to what would have been expected from the Doering–Zeiss hypothesis, which held that the structure corresponding to the activated complex for a coupled process was transformed into the intermediate species of similar structure in an uncoupled process, if the latter were made specially favorable by structural or environmental modifications.[49] Thus, the two structures (and the two mechanisms) could not coexist. More O'Ferrall[50] therefore constructed, in the form of contour maps, "a model...which is shown...to describe correctly the borderline between the concerted and stepwise mechanisms." More O'Ferrall's maps naturally refer to elimination reactions; they therefore show carbon–hydrogen stretching as the abscissa and carbon-leaving group stretching as the ordinate. The maps were constructed again purely on the basis of ratiocination. The purpose of these maps was to account for the "borderline" elimination reaction mentioned above, in which it appeared that two mechanisms were simultaneously operative: (1) an uncoupled, anionic (E1cb) pathway and (2) a coupled (E2) pathway. In achieving such a surface, More O'Ferrall built in several triple-minimum potentials of the sort considered by Albery to be unlikely. Now this system is more complicated than the double-proton-transfer systems Albery was treating, and we will consider below the chances of actually having triple-minimum potentials in complex aggregates. At this point, we note that such potentials are an absolute necessity if one is to represent a case in which cationic and anionic intermediates exist at potential minima, *and* a coupled pathway also exists.

In our calculations, coupled and uncoupled pathways have not been found to coexist, the prerequisite for coupling being loss of one of the intermediates as a stable species. Our findings to date therefore favor a "modified Doering–Zeiss" picture in which the disappearance of an intermediate as a stable entity generates an activated complex for a related, kinetically coupled process.

The major effort to form two-dimensional contour maps on the basis of chemical reasoning and to apply them to the solution of mechanistic problems has been that of Jencks.[51] Jencks lays down a prescription for constructing these diagrams from stated assumptions. The resulting diagrams are used to interpret the vast array of mechanistic data on general acid–base catalysis in water and to derive this general rule: "Concerted[52] general acid–base catalysis...can occur only (a) at sites that undergo a large change in pK in the course of the reaction, and (b) when...the pK of the catalyst is intermediate between the initial and final pK values of the substrate site."[54]

Jencks' guidelines for diagram construction exclude any potentials, except single- and double-minimum potentials along lines parallel to the axes, but the figures show that triple minima are allowed to enter along the cation–anion diagonals (Figures 1, 3, 5, and 6 of ref 51). Indeed, this is the only way in which a dynamically coupled pathway can possibly exist and compete with dynamically and kinetically uncoupled pathways ("stepwise" in Jencks terminology) through existing intermediates. Users of such diagrams should be aware of this and should provide a physical rationale for the special stability which has to be associated with the coupled activated complex in order for the third minimum to be generated.

In the surfaces generated in our study, coupled pathways arose only when at least one of the intermediates was nonexistent as a chemical species (thus, when the reactant–intermediate potential had become a single-minimum potential). Jencks arrives at a closely related conclusion: "...concerted mechanisms are more likely to be found in reactions in which there is no significant free-energy barrier for one or the other step. When this is the case the intermediates have no finite existence...."

Two authors have attempted to put these kinds of consideration into quantitative form, not by use of quantum mechanics, but by employing pragmatically derived functions to generate energy surfaces. Critchlow[55] generated his surfaces by using experimental pK's to estimate relative energies of reactants, products, and

(47) E. R. Thornton, *J. Amer. Chem. Soc.*, **89**, 2915 (1967).

(48) G. C. Swain and E. R. Thornton, *J. Amer. Chem. Soc.*, **84**, 817 (1962).

(49) W. E. Doering and H. H. Zeiss, *J. Amer. Chem. Soc.*, **75**, 4733 (1953). This "structural hypothesis" was advanced to unite the mechanistic pictures for SN1 (uncoupled) and SN2 (coupled) displacement reactions; *cf.* A. Streitwieser, Jr., "Solvolytic Displacement Reactions," McGraw-Hill, New York, N. Y., 1962, pp 66–92. It can be equally applied to elimination or any other process in which the coupling question arises (see below).

(50) R. A. More O'Ferrall, *J. Chem. Soc. B*, 274 (1970). In this paper, references to the underlying experimental work are given.

(51) W. P. Jencks, *Chem. Rev.*, 72, 705 (1972).

(52) By "concerted" Jencks means "that the rate-determining transition state occurs in the central region of the diagram with significant movement along both coordinates...."[53] In our terminology this is a dynamically and kinetically coupled pathway.

(53) See ref 51, p 707.

(54) This rule [previously described in W. P. Jencks, *J. Amer. Chem. Soc.*, **94**, 4731 (1972)] is often known as the Libido Rule, presumably because it describes the forces leading to coupling. Both parts of the Libido rule translate roughly into the language of this article as, "A dynamically and kinetically coupled reaction can occur only if both the cationic and anionic intermediates are unstable with respect to reactants and products."

(55) J. E. Critchlow, *J. Chem. Soc., Faraday Trans. 1*, **68**, 1774 (1972).

intermediates, by assuming a linear change in energy along each edge of the surface and by using a plausible formula relating the edge potentials to points in the central region of the surface. Since his edge potentials are linear, all his intermediates have no stable existence and all mechanisms are coupled. When we apply Critchlow's formulas for the location of the transition state to our medium surfaces, we find poor agreement. This doubtlessly results from the use of experimental pK's, which do not properly represent relative energies in the context of our calculations.[40]

Dunn[56] used fourth-order polynomials to generate plausible edge potentials and combined these by assuming that each edge potential contributed to a point on the surface in inverse proportion to the distance of the point from the edge. Dunn's particular interest was the application of these surfaces to questions of transition-state structure in acetal hydrolysis. All of his calculated surfaces, except for one, favor uncoupled ("stepwise") mechanisms, and none shows a triple-minimum potential on the cation–anion diagonal. The one surface which favors a coupled mechanism shows a single-minimum potential along the cation–anion diagonal. In this case, the edge potentials have been chosen so that the intermediates are at energy plateaus rather than minima.

As we have already noted, the triple-minimum cation–anion diagonal plays a crucial role in potential surfaces which represent competing coupled and uncoupled processes. Such a potential has not appeared in any of our calculations to date and is difficult to envision. Some special stabilization of the coupled activated complex would be required, and a potential source of such stabilization cannot readily be suggested. More complex systems are currently under study, and we shall reserve judgment on this point until that work is complete. Nevertheless, it is worth noting that it has been questioned whether coupled processes ever exist in systems where the intermediates of the uncoupled routes are capable of attainment.[57]

Future Studies. The continuation of this work will be directed toward exploring the generality of the conclusions reached on the basis of these simple model systems. Besides the use of *ab initio* techniques to check the results for a few of the surfaces, new systems to be examined will include asymmetric systems in which proton donors and acceptors differ, unsaturated systems, and larger aggregates to illuminate the role of environmental influences. Calculations are also envisioned for proton transfers to and from carbon and processes in which bonds among heavy atoms are formed and broken (with appropriate consideration of correlation effects).

Acknowledgments. We are happy to thank Douglas R. Freeman and G. Michael Henry for their expert technical assistance, Professor Marlin Harmony for useful discussions, and the personnel of the Computation Center of the University of Kansas for their cooperation during the course of the calculations. We are also grateful to Dr. B. M. Dunn for sending us a copy of his paper before its publication.

(56) B. M. Dunn, *Int. J. Chem. Kinet.*, **6**, 143 (1974).

(57) F. G. Bordwell, *Accounts Chem. Res.*, **3**, 281 (1970). Bordwell examines rigorously the evidence for coupling in several reactions, some widely believed to be coupled, and concludes that it is insufficient.